

## Structure and Conformational Dynamics of Trichothecene Mycotoxins

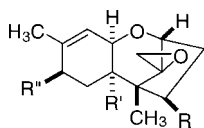
Wayne E. Steinmetz,\* Paul Robustelli, Eric Edens, and David Heineman

Chemistry Department, Pomona College, Claremont, California 91711

Received October 5, 2007

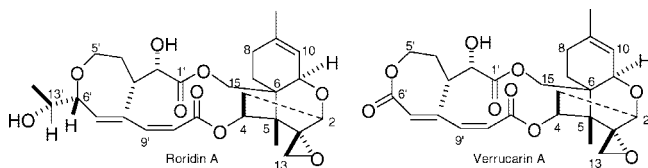
A combination of NMR spectroscopy and molecular modeling has been employed to characterize the conformation and dynamics of the macrolide ring in verrucarin A and roridin A, two closely related toxins in the trichothecene mycotoxin family. Longitudinal carbon-13 relaxation times demonstrate the relative flexibility of the macrolide ring. The calculations, NOEs, and scalar vicinal coupling constants show that verrucarin A in CDCl<sub>3</sub> and CD<sub>2</sub>Cl<sub>2</sub> predominantly adopts a single, well-defined conformation that matches the crystal structure. In contrast, roridin A is present as a mixture of two conformers.

Trichothecene mycotoxins are highly toxic substances that are produced by a range of fungi in the family *Hypocreaceae* including the genera *Fusarium*, *Trichoderma*, and *Myrothecium*.<sup>1</sup> They have been responsible for the lethal contamination of grains and ventilation systems via dust and hay and have been claimed as components of yellow rain, a chemical agent used by the Soviet army in Afghanistan and Southeast Asia.<sup>1,2</sup> Their covalent structure has been well characterized, and several crystal structures have been published.<sup>3</sup> They are a class of sesquiterpenes with a characteristic trichothecene nucleus, a rigid tetracyclic ring system.



The double bond and the epoxide group in the trichothecene nucleus are responsible for the biological activity of the toxins.<sup>4</sup> Trichothecene toxins are believed to act by binding to the 60S subunit of the ribosome and thus inhibiting protein synthesis.<sup>4</sup>

The attachment of a macrolide ring to the R' and R'' positions greatly increases the toxicity, and the class of macrolide toxins are among the most toxic.<sup>2</sup> These compounds are conformationally interesting because of the potential flexibility of the larger ring. Verrucarin A and roridin A, which are produced by fungi from the genus *Myrothecium*, are representatives of the macrolide toxins.



Their covalent structures were determined by the Tamm group at the University of Basel.<sup>5,6</sup> X-ray crystal structures confirmed their stereochemistry and established their conformation in the solid state.<sup>7–9</sup> We initiated this study to provide via NMR spectroscopy and molecular modeling complementary information on their solution-phase conformation with a view that the results might provide insight into their biological activity. The comparison of the results of the two toxins is instructive, as they differ only at C-6'.

The early use of NMR spectroscopy in the determination of the structure and conformation of trichothecene mycotoxins, based entirely on one-dimensional methods, dates back to the classic work

of Tamm's group.<sup>5,6,10</sup> Recent studies have employed 1D and 2D NMR methods in the assignment process of a range of mycotoxins but not roridin A and verrucarin A.<sup>11,12</sup> Our complete assignment of the spectra of roridin A and verrucarin A in CDCl<sub>3</sub> (Table 1) is based on the standard portfolio of methods including COSY, ROESY, HMQC, and HMBC.<sup>13</sup> Our carbon assignment agrees with the earlier, tentative assignment of Breitenstein and Tamm with one exception, a reversal for carbonyl carbons 6' and 11' of verrucarin A.

NMR spectroscopy is a powerful tool for the determination of the solution-phase, three-dimensional structure of complex molecules.<sup>14,15</sup> NMR constraints on the structure include scalar vicinal coupling constants and NOEs. Structures are calculated by combining the NMR constraints with a molecular mechanics force field that accurately models bond lengths, bond angles, and van der Waals forces. The determination of a structure or conformation becomes in effect a fit of the data in torsional space. If the molecule adopts a single conformation or a narrow range of very similar conformations, the conformation is generated by constrained molecular mechanics. The constraints are added to the force field via a penalty function, and the three-dimensional structure is defined by those conformations that satisfy all the NMR constraints and yield a low energy. This approach has been employed in NMR studies of the conformation of erythromycin derivatives.<sup>16,17</sup> A different strategy is required if all the NMR constraints cannot be fit to a single conformation or structure. In this case, one employs unconstrained molecular dynamics to generate a library of conformers and assigns features in the NMR spectra to the low-energy conformers.<sup>18</sup> We adopted this approach early in this study when we discovered that the cross-peaks in the ROESY spectrum of roridin A could not be assigned to a single conformation. Although all the NMR constraints for verrucarin A are consistent with a single conformation, we applied the latter approach to it as well so that roridin A and verrucarin A were handled in the same manner.

The modeling component of our conformational analysis had the following steps: an exhaustive search of conformational space, the calculation of the structures and energies of low-energy conformers at a high level of theory, and calculation of NMR parameters. The Random Search algorithm of SYBYL was used for the conformational search. This method was found to be highly effective in our study of erythromycin analogues, which is also a system with a macrolide ring.<sup>16,17</sup> Crystal structures of verrucarin A<sup>7</sup> and roridin A<sup>9</sup> provided the seed structures for the search. In each cycle, a subset of bonds is randomly chosen and each torsional angle is also set randomly. The selection step is followed by a molecular mechanics minimization with the 1994 version of the Merck molecular force field (MMFF). This Class II force field has been shown to yield excellent results.<sup>19,20</sup> By completing this process for thousands of cycles, we identified with confidence a

\* Corresponding author. Tel: 909-621-8447. Fax: 909-607-7726. E-mail: wsteinmetz@pomona.edu.

**Table 1.** NMR Data for Verrucaric Acid and Roridin A in CDCl<sub>3</sub> at 25 °C<sup>a</sup>

| C#     | verrucarin A     |            |              | roridin A        |            |              |
|--------|------------------|------------|--------------|------------------|------------|--------------|
|        | $\delta_H$       | $\delta_C$ | $T_{1C}$ (s) | $\delta_H$       | $\delta_C$ | $T_{1C}$ (s) |
| 2      | 3.84             | 78.9       | 0.82 ± 0.058 | 3.83             | 79.3       | 0.61 ± 0.033 |
| 3      | 2.21(a), 2.46(b) | 34.9       | 0.42 ± 0.072 | 2.19(a), 2.42(b) | 35.1       | 0.36 ± 0.035 |
| 4      | 5.79             | 75.5       | 0.80 ± 0.026 | 5.76             | 74.5       | 0.66 ± 0.025 |
| 5      |                  | 49.5       |              |                  | 49.6       |              |
| 5-Me   | 0.83             | 7.3        |              | 0.79             | 7.7        |              |
| 6      |                  | 44.2       |              |                  | 44.0       |              |
| 7      | 1.67(a), 1.88(b) | 20.0       | 0.44 ± 0.048 | 1.75(a), 1.90(b) | 20.5       | 0.64 ± 0.027 |
| 8      | 1.91(a), 1.96(b) | 27.5       | 0.40 ± 0.041 | 1.81(a), 2.04(b) | 27.9       | 0.32 ± 0.032 |
| 9      |                  | 141.2      |              |                  | 141.2      |              |
| 9-Me   | 1.73             | 23.3       |              | 1.75             | 23.5       |              |
| 10     | 5.41             | 117.9      | 0.82 ± 0.048 | 5.41             | 118.5      | 0.67 ± 0.040 |
| 11     | 3.54             | 66.9       | 0.90 ± 0.058 | 3.57             | 67.4       | 0.78 ± 0.064 |
| 12     |                  | 65.2       |              |                  | 65.4       |              |
| 13     | 2.78(a), 3.1(b)  | 47.8       | 0.36 ± 0.051 | 2.77(a), 3.10(b) | 48.0       | 0.29 ± 0.042 |
| 15     | 4.20(a), 4.78(b) | 63.5       | 0.43 ± 0.070 | 4.42             | 64.8       | 0.73 ± 0.032 |
| 1'     |                  | 174.7      |              |                  | 175.1      |              |
| 2'     | 4.12             | 74.2       | 1.06 ± 0.030 | 4.07             | 75.8       | 0.86 ± 0.052 |
| 2'-OH  | 2.63             |            |              | 2.85             |            |              |
| 3'     | 2.33             | 33.2       | 0.96 ± 0.046 | 2.03             | 37.4       | 0.82 ± 0.044 |
| 3'-Me  | 0.86             | 33.2       |              | 1.09             | 14.7       |              |
| 4'     | 1.78(a), 1.94(b) | 32.2       | 0.47 ± 0.051 | 1.58(a), 1.84(b) | 33.3       | 0.37 ± 0.040 |
| 5'     | 3.96(a), 4.49(b) | 61.1       | 0.48 ± 0.082 | 3.51             | 70.1       | 0.37 ± 0.042 |
| 6'     |                  | 165.4      |              | 3.63             | 84.3       | 0.82 ± 0.029 |
| 7'     | 6.02             | 127.5      | 0.78 ± 0.047 | 5.97             | 139.4      | 0.60 ± 0.040 |
| 8'     | 8.02             | 138.8      | 0.74 ± 0.036 | 7.64             | 126.3      | 0.61 ± 0.030 |
| 9'     | 6.65             | 138.9      | 0.74 ± 0.032 | 6.62             | 144.1      | 0.59 ± 0.025 |
| 10'    | 6.13             | 125.8      | 0.78 ± 0.028 | 5.78             | 117.8      | 0.68 ± 0.027 |
| 11'    |                  | 166.1      |              |                  | 166.7      |              |
| 13'    |                  |            |              | 3.58             | 71.1       | 0.87 ± 0.022 |
| 13'-Me |                  |            |              | 1.20             | 18.5       |              |
| 13'-OH |                  |            |              | 2.70             |            |              |

<sup>a</sup> Measured at 400 MHz (<sup>1</sup>H) and 100 MHz (<sup>13</sup>C). The uncertainties for  $T_1$  are at the 95% confidence level. In the standard enumeration scheme, the methyl carbons attached to carbons 5, 9, 3', and 13' are given carbon numbers 14, 16, 12', and 14', respectively.

**Table 2.** Values of  $nT_1(\text{adj})$  for Verrucaric Acid and Roridin A in CDCl<sub>3</sub> at 25 °C

| carbons                 | verrucarin A           | roridin A              |
|-------------------------|------------------------|------------------------|
|                         | $nT_1(\text{adj})$ (s) | $nT_1(\text{adj})$ (s) |
| 2, 3, 4, 10, 11, 7'-10' | 0.80 ± 0.04            | 0.67 ± 0.06            |
| 2', 3', 4', 5'          | 1.01 ± 0.06            | 0.82 ± 0.06            |

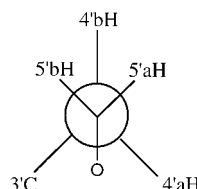
**Table 3.** Diagnostic Interproton Distances for Verrucaric Acid from the 500 ms ROESY Spectrum

| proton pair | strength of ROE <sup>a</sup> | $r_{HH}$ (Å) <sup>b</sup> |
|-------------|------------------------------|---------------------------|
| 4H-15bH     | S                            | 1.91                      |
| 11H-15aH    | M                            | 2.70                      |
| 11H-15bH    | M                            | 2.48                      |
| 2'H-7aH     | W                            | 3.75                      |
| 2'H-4'aH    | S                            | 2.36                      |
| 2'H-4'bH    | W                            | 3.03                      |
| 3'H-5'bH    | W                            | 3.23                      |
| 3'Me-5'bH   | M                            | 2.85                      |
| 3'H-8'H     | M                            | 2.73                      |
| 7'H-9'H     | M                            | 2.53                      |
| 8'H-5Me     | W                            | 4.09                      |
| 7'H-9'H     | M                            | 2.53                      |

<sup>a</sup> The strength of the ROE was obtained from the volume of the cross-peak in the 500 ms ROESY spectrum in CDCl<sub>3</sub> at 25 °C. S corresponds to  $r_{HH} < 2.5$  Å; M, to  $2.5$  Å  $< r_{HH} < 3.0$  Å; W, to  $3.0$  Å  $< r_{HH} < 4.0$  Å. <sup>b</sup> The interproton distances  $r_{HH}$  are from the global minimum structure generated by the modeling calculations. In the case of an ROE between a proton X and protons Y on a methyl group, the distance between proton X and the methyl carbon is given.

complete set of conformers with low energies, i.e., within 17 kJ/mol of the global minimum. Conformers in this energy range constitute 99.9% of all conformers at 298 K. *Ab initio* quantum mechanics was applied in a second round of geometry optimization. In order to achieve an optimal ranking of the low-energy conform-

**Table 4.** Vicinal Coupling Constants of Verrucaric Acid and Torsional Angles

| torsional angle   |  |                                |                                |                                |
|-------------------|---|--------------------------------|--------------------------------|--------------------------------|
|                   | $\varphi(\text{xls})^a$ (deg)   | $\varphi(\text{calc})^b$ (deg) | $^3J_{HH}(\text{expt})^c$ (Hz) | $^3J_{HH}(\text{calc})^d$ (Hz) |
| 8'H-8'C-9'C-9'H   | 176.2   | 177.8                          | 11.7                           | 11.1                           |
| 4'aH-4'C-5'C-5'aH | 48.6  | 51.8                           | 5.2                            | 5.1                            |
| 4'aH-4'C-5'C-5'bH | 168.5   | 172.9                          | 12.1                           | 11.6                           |
| 4'bH-4'C-5'C-5'aH | 293.1   | 296.3                          | 2.6                            | 1.6                            |
| 4'bH-4'C-5'C-5'bH | 53.0  | 57.3                           | 3.3                            | 2.7                            |
| 3'H-3'C-4'C-4'aH  | 60.0  | 62.9                           | 4                              | 2.8                            |
| 3'H-3'C-4'C-4'bH  | 176.3   | 179.4                          | 11.5                           | 11.7                           |
| 2'H-2'C-3'C-3'H   | 289.0   | 296.2                          | 2                              | 1.7                            |

<sup>a</sup> Torsional angles in the crystal structure. <sup>b</sup> Torsional angles in the calculated global minimum structure. <sup>c</sup> Experimental coupling constant in CD<sub>2</sub>Cl<sub>2</sub> at 25 °C. <sup>d</sup> Coupling constants calculated from the global minimum structure.

ers, we used density functional theory (DFT) with a 6-31G(d,p) basis set and an mPW1PW91 functional, which includes Hartree-Fock exchange with an analytically derived parameter.<sup>21</sup> DFT calculations of conformational energy differences have a mean error of 1.3 kJ/mol at this level.<sup>20</sup> By applying Boltzmann statistics at 298 K to the results of the *ab initio* calculations, we found that more than 90% of the toxin was present as either one (verrucarin A) or two (roridin A) conformer(s). In a final round of calculations on these three species, the GIAO method was employed to obtain chemical shifts and scalar coupling constants.<sup>22</sup> Average coupling

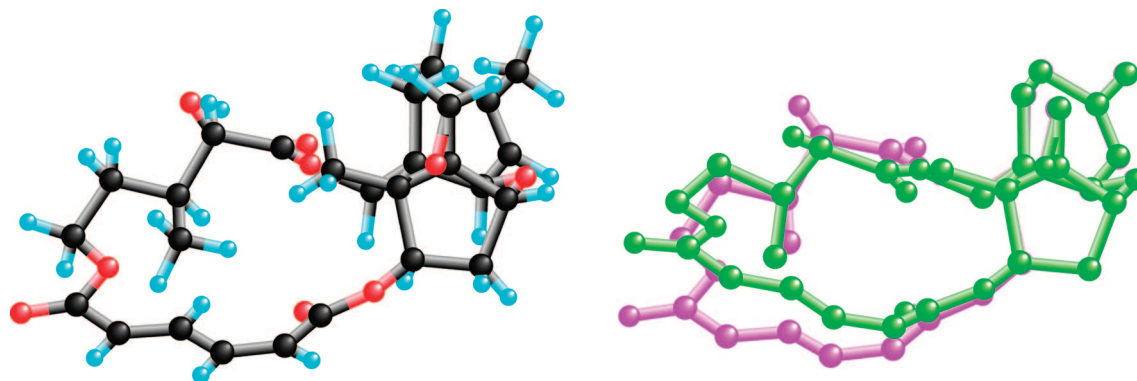


**Figure 1.** Three-dimensional structure of verrucaric acid. Left: the global minimum conformer calculated using DFT. Right: overlay of the global minimum (magenta) with the crystal structure (green). Only the heavy atoms are shown.

**Table 5.** Diagnostic Interproton Distances for Roridin A from the 500 ms ROESY Spectrum

| proton pair <sup>a</sup> | strength of ROE | $r_{HH}$ (Å)         |                       |
|--------------------------|-----------------|----------------------|-----------------------|
|                          |                 | conf. I <sup>b</sup> | conf. II <sup>c</sup> |
| 4H–15bH                  | S               | 1.89                 | 1.92                  |
| 11H–15bH                 | S               | 2.42                 | 2.59                  |
| 2'H–3'H                  | S               | 2.43                 | 2.52                  |
| <b>2'H–4'bH</b>          | S               | 2.34                 | 3.72                  |
| <b>3'H–5Me</b>           | M               | 3.67                 | 5.75                  |
| 3'H–5'aH                 | S               | 2.45                 | 2.17                  |
| <b>3'H–8'H</b>           | S               | 2.63                 | 5.17                  |
| 4'aH–8'H                 | S               | 4.43                 | 2.50                  |
| 4'bH–8'H                 | W               | 5.54                 | 3.69                  |
| 4'bH–5Me                 | M               | 4.49                 | 3.67                  |
| <b>5'aH–8'H</b>          | S               | 2.65                 | 3.94                  |
| 5'bH–8'H                 | S               | 3.99                 | 2.67                  |
| 7'H–9'H                  | S               | 2.36                 | 2.44                  |
| <b>8'H–3'Me</b>          | M               | 3.38                 | 4.61                  |

<sup>a</sup> Normal font, the constraint is satisfied by both conformers; bold face, only by conformer I; italics, only by conformer II. <sup>b</sup> Interproton distance for conformer I, the global minimum. <sup>c</sup> Interproton distance for conformer II, the species 0.6 kJ/mol higher in energy.

**Table 6.** Vicinal Homo- and Heteronuclear Coupling Constants of Roridin A and Torsional Angles

| torsional angle   | conformer I     |                         | conformer II    |                         | average                 |                          |
|-------------------|-----------------|-------------------------|-----------------|-------------------------|-------------------------|--------------------------|
|                   | $\varphi$ (deg) | $^3J(\text{calc})$ (Hz) | $\varphi$ (deg) | $^3J(\text{calc})$ (Hz) | $^3J(\text{calc})$ (Hz) | $^3J(\text{exp})^a$ (Hz) |
| 4'aH–4'C–5'C–5'aH | 180.9           | 11.2                    | 55.0            | 5.9                     | 8.9                     | 9.2                      |
| 4'aH–4'C–5'C–5'bH | 298.7           | 3.4                     | 174.7           | 10.6                    | 6.6                     | 5.9                      |
| 4'bH–4'C–5'C–5'aH | 295.0           | 1.9                     | 170.8           | 11.1                    | 6.0                     | 7.1                      |
| 4'bH–4'C–5'C–5'bH | 52.8            | 2.9                     | 290.4           | 3.4                     | 3.1                     | 2.5                      |
| 3'H–3'C–4'C–4'aH  | 199.7           | 8.6                     | 178.3           | 11.0                    | 9.7                     | 10.5                     |
| 3'H–3'C–4'C–4'bH  | 83.6            | 0.7                     | 61.2            | 3.2                     | 1.8                     | 2.6                      |
| 2'H–2'C–3'C–3'H   | 301.9           | 2.4                     | 76.6            | 2.9                     | 2.6                     | 3.2                      |
| 11'C–O–4C–4H      | 327.8           | 3.8                     | 329.6           | 3.9                     | 3.8                     | 3.7                      |
| 5'C–4'C–3'C–3'H   | 324.4           | –0.1                    | 300.0           | 1.3                     | 0.5                     | ≈0                       |
| 2'C–3'C–4'C–4'aH  | 83.8            | –3.0                    | 66.5            | –3.1                    | –3.0                    | ≈0                       |

<sup>a</sup> Experimental coupling constant in CD<sub>2</sub>Cl<sub>2</sub> at 25 °C.

constants, which could be compared with the experimental results, were calculated via Boltzmann averaging.

## Results and Discussion

Fifty thousand cycles of the Random Search algorithm followed by energy minimization generated the global minimum of the two mycotoxins and 45 low-energy, i.e., within 84 kJ/mol of the global minimum, conformations for verrucaric acid and 104 for roridin A. The conformer count indicates that the macrolide ring in roridin A is more flexible. This conclusion is supported by the distribution of conformers. Roridin A has 18 conformers within 17 kJ/mol of the global minimum and verrucaric acid only five. An analysis of the conformations showed that conformational flexibility resides in the following dihedral angles in the macrolide ring: O–15C–6C–5C, O–1'C–2'C–3'C, 1'C–2'C–3'C–4'C, 2'C–3'C–4'C–5'C, 3'C–4'C–5'C–O, 4'C–5'C–O–6'C, and 5'C–O–6'C–7'C. In addition, the orientation of the C–6' CH<sub>3</sub>OHCH– group of roridin A makes a contribution to its conformational energy. Consequently, a single gauche ( $\varphi[13'H–13'C–6'C–6'H] \approx -60^\circ$ ) conformation of the group was used in the DFT calculations so that energy changes would reflect solely changes in the macrolide ring.

The modeling result of relative inflexibility in the trichothecene nucleus and flexibility in the 1'–6' section of the macrolide ring is supported by the chemical shift data. The carbon shifts primarily provide information on the covalent structure, and the experimental shifts correlate well, i.e.,  $R > 0.998$ , with those calculated from quantum mechanics. Conformationally the proton chemical shifts are more interesting. In contrast to the relative invariance of the proton shifts on the trichothecene nucleus, the 2' through 5' shifts change significantly upon modification of the macrolide ring. The 5'-methylene protons are particularly striking. In the verrucaric acid structure calculated via modeling and also observed in crystallography, they are oriented above and below the macrolide ring and the change in chemical environment translates to an observed and calculated difference,  $\delta_{5'b} - \delta_{5'a}$ , of 0.53 and 0.79 ppm, respectively. In contrast, the 5'-methylene protons are observed to be degenerate in the case of roridin A; this degeneracy suggests conformational averaging. The modeling calculations yielded significant differences for the two dominant conformers,  $\delta_{5'b} - \delta_{5'a} = -0.41$  and 0.19 ppm, but a Boltzmann average of only  $-0.15$  ppm.

The increased flexibility of the macrolide ring in roridin A is a natural consequence of bonding theory. In the case of verrucaric acid, the conjugation of atoms C–6' through C–11' confers rigidity to this segment of the macrolide ring. The extended, nearly planar conformation yielded by the modeling calculations is validated by  $^3J_{8H,9H} = 11.7$  Hz. The magnitude of the coupling constant demonstrates an anti conformation between H–8' and H–9'. Large values, i.e.,  $^3J > 10.7$  Hz, were observed in a study of conjugated polyene aldehydes and ketones where rotational constants derived from their microwave spectra clearly demonstrated an extended conformation.<sup>23</sup> With roridin A, the hybridization of C–6' is sp<sup>3</sup> instead of sp<sup>2</sup> and the scope of the conjugated system is reduced

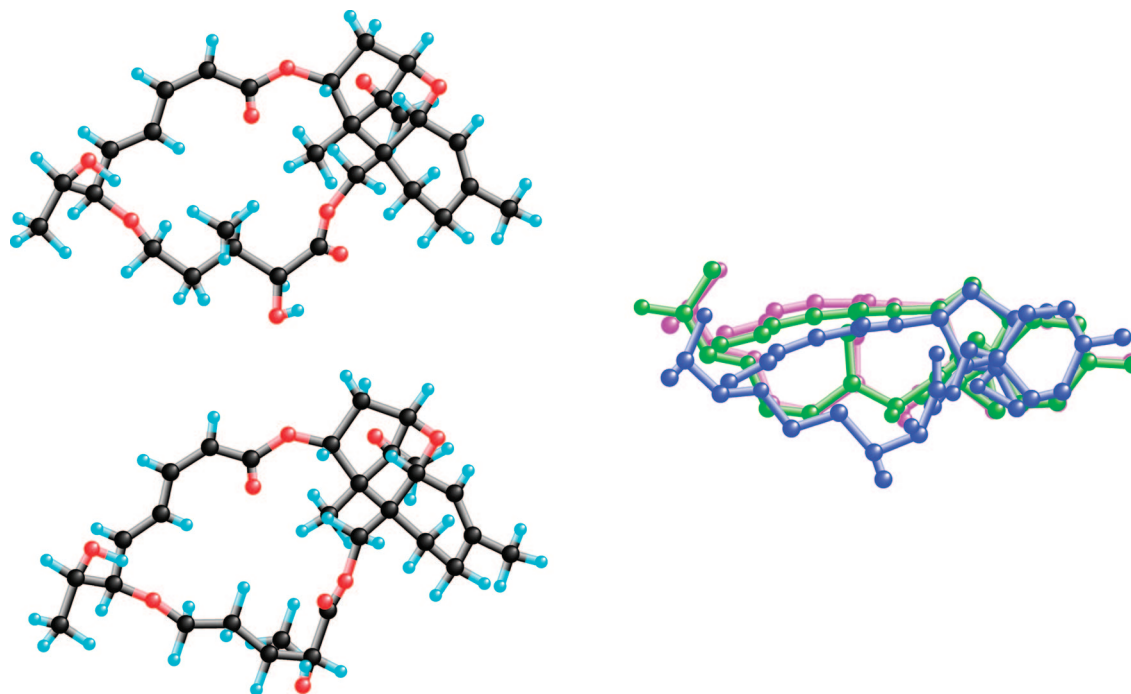


**Figure 2.** Three-dimensional structure of roridin A. Left: the two principal conformers generated by the DFT calculations, conformer I (the global minimum) at the top and conformer II at the bottom. Right: overlay of conformer I (magenta) and conformer II (blue) with the crystal structure (green). Only the heavy atoms are seen.

with a resulting increase in flexibility around C-6'. The section where conjugation is preserved maintains an anti, extended conformation, as shown by the value of  ${}^3J_{8\text{H},9\text{H}}$ , 11.5 Hz.

The values of carbon  $T_1$  in Table 1, which were acquired by the inversion–recovery pulse sequence with proton decoupling, provide further semiquantitative information on relative flexibility of the molecule. As elaborated by Abragam, relaxation measured by  $T_1$  requires a random modulation of the magnetic field experienced by a carbon spin.<sup>24</sup> For our oxygen-free samples, the source of the interaction is the coupling of the carbon magnetic dipole with dipoles from all neighboring protons. The effectiveness of each carbon–proton interaction depends inversely on the sixth power of the carbon–proton distance, and therefore  $T_1$  is dominated in the case of all but the quaternary carbons by the proton(s) directly bonded to the carbon. In order to compare  $T_1$ 's, two adjustments are needed. Using the structure of the molecule, the small contribution from nonbonded protons to  $T_1$  is subtracted. The adjusted  $T_1$ ,  $T_1(\text{adj})$ , now depends solely on the directly bonded hydrogens. A methylene carbon will relax twice as fast as a methine carbon, so in a second adjustment,  $T_1(\text{adj})$  is multiplied by the number of bonded hydrogens,  $n$ . The distribution of the values of  $nT_1(\text{adj})$  for each mycotoxin into two groups (Table 2) is a consequence of relaxation theory. The relaxation rate depends on the frequency of the modulation of the dipole–dipole interaction. In the case of a rigid rotor, the overall rotation of the molecule is the sole source of the modulation. However, real molecules vibrate, and for small molecules such as the mycotoxins, large-amplitude vibrational motions have the effect of increasing  $T_1$ . We note that for each mycotoxin  $nT_1(\text{adj})$  is greater for the more flexible regions of the molecule. Also  $nT_1(\text{adj})$  is systematically shorter for roridin A. The substituent at C-6' has the hydrodynamic effect of slowing down the rotation of the entire molecule and reducing the frequency of the dipole–dipole modulation.

DFT calculations on the five lowest-energy conformers showed that verrucaridin A is present predominantly as one conformer. The conformer closest in energy lies 7.8 kJ/mol above the global minimum with a corresponding Boltzmann population of 0.04 mol %. In contrast, the more flexible roridin A is present as two, nearly equi-energetic species. The energy difference between these two

species is 0.6 kJ/mol. Both DFT and molecular mechanics with the Merck molecular force field yielded the same ordering of conformers, and we are confident in the robustness of the result.

The calculated structure of the predominant verrucaridin A conformer is validated by the NMR data. The 500 ms ROESY spectrum, which provides upper bounds on interproton distances, yields a set of 10 diagnostic cross-peaks between protons across the ring (Table 3). All ROESY cross-peaks are consistent with the structure. The ROESY data are complemented by a set of vicinal scalar coupling constants (Table 4). If one uses NMR data to define the conformation, the coupling constants must be used conservatively. First the parameters describing their dependence on torsional angle depend on factors such as the nature of the substituents.<sup>25</sup> Small and large coupling constants have an unambiguous interpretation as they correspond to roughly gauche and anti conformations. There are multiple interpretations to intermediate values. However, in this study we are using the coupling constants to validate our conformational analysis. Coupling constants can be reliably calculated using DFT, and the excellent agreement between the observed and calculated coupling constants provides convincing support for the calculated structure.

The three-dimensional structure of the global minimum conformer of verrucaridin A, calculated via DFT and validated with the NMR data, is shown in Figure 1. It matches well although not perfectly the crystal structure. The torsional angles defining the conformation of the macrolide ring agree well; the standard deviation of their difference,  $s(\text{torsion})$ , is  $6.8^\circ$ . An overlay of the two structures is also shown in Figure 1. Using the backbone atoms in the trichothecene nucleus, the root-mean-square distance between atoms in the two structures (rms) is  $0.029 \text{ \AA}$ . However, if the backbone atoms in the macrolide ring are included in the fit, the rms increases to  $0.31 \text{ \AA}$ . A visual examination of the overlay shows the nearly perfect alignment of the trichothecene nucleus but a difference in the orientation of the plane defined by the carbon and oxygen atoms in the macrolide ring. This difference between the structures is determined for the most part by the C6–C15–O–C1' and C9'–C10'–C11'–O torsional angles.

The NMR data provide striking confirmation of the modeling results for roridin A. Neither of the nearly equi-energetic conform-

ers, referred to as I and II, is sufficient to explain the ROESY data tabulated in Table 5, but every ROESY cross-peak can be assigned to one or both of the conformers. Comparable support for the presence of both conformers is provided by the coupling constants (Table 6). The Boltzmann average of the calculated coupling constants, which were found to be independent of temperature over the range  $-50$  to  $32$  °C, matches the experimental data, whereas the calculated values for either species do not.

The 3D structures of the two roridin A conformers as well as their overlays with the crystal structure are shown in Figure 2. The global minimum closely matches the crystal structure. The rms for the pair of structures is  $0.13$  Å and  $s(\text{torsion})$  is  $3.8^\circ$ . The other structure is distinctly different, visually as shown in Figure 2 and quantitatively with an rms of  $0.56$  Å and  $s(\text{torsion})$  of  $44^\circ$ . Two torsional angles,  $1'C-2'C-3'C-4'C$  and  $3'C-4'C'-5'C-O$ , make the largest contributions to the difference in structure.

An issue accompanying any structural study is the relation of structure to activity. The epoxide group in the trichothecene nucleus is required for biological activity, but the conformation of the molecule must be invoked to understand the large variation in activity among the mycotoxins.<sup>2</sup> Handling this quantitatively, the science of QSAR, is a nontrivial enterprise, and a successful model must address not only binding in the active site of the enzyme associated with the toxin's activity but also the issues of ADME.<sup>26</sup> The dependence of the octanol-water partition coefficient, a frequently used QSAR parameter, on molecular structure raises the hope for biological relevance of our conformational analysis.<sup>27</sup>

We applied the QSAR methodology to four published data sets in which the range of toxins studied was broad enough to yield a change in biological activity by several orders of magnitude. A wide range in the dependent variable is usually a condition for the successful derivation of a QSAR. The studies examined the effect of mycotoxins on the K-562 human cell line,<sup>28</sup> the lethal intraperitoneal LD<sub>50</sub> with mice,<sup>29</sup> the superinduction of interleukin-5 in murine CD4<sup>+</sup> cells,<sup>30</sup> and relative toxicity to mice.<sup>2,31</sup> The data sets ranged in size from five to eight compounds. In each case, we found a statistically significant correlation of the logarithm of a measure of biological activity such as LD<sub>50</sub> with the number of valence electrons, NVE. NVE has been shown to be an excellent proxy for molecular polarizability, a QSAR parameter.<sup>32</sup> This result, satisfying to the medicinal chemist, addresses the large variation in toxicity over a broad range of mycotoxins, but does not reveal a direct correlation with molecular conformation. We are hopeful that an examination of a larger database will demonstrate the role of conformation in the biological activity of mycotoxins. A worthy candidate for this future quest is the data set of 26 macrolide mycotoxins examined by Jarvis et al.<sup>33</sup> This study has shown that modeling calculations perform well in the generation of conformers and modeling without NMR spectroscopy can be employed in the analysis of Jarvis' database.

## Experimental Section

**Molecular Modeling.** Some preliminary work was done using the Version '06 of Spartan (Wavefunction, Inc., Irvine, CA). Version 7.2 of SYBYL (Tripos, Inc., St. Louis, MO) was the primary tool for molecular mechanics and analysis of the structures. A full description of the strategy of the modeling calculations is provided in our papers on derivatives of erythromycin.<sup>16,17</sup> SYBYL provides a range of options for searching conformational space. Following our success with erythromycin, an exhaustive search of conformational space was performed with 50 000 cycles of the Random Search algorithm. Random Search parameters were set to default values with the following exceptions: Bump Factors, 0.02; Ring Bond closure,  $10$  Å; energy cutoff,  $418$  kJ/mol. All *ab initio* calculations were performed using version 03 of Gaussian (Gaussian, Inc., Pittsburgh, PA).

**NMR Spectroscopy.** Samples of the mycotoxins were purchased from Sigma and used without further purification. Solutions ( $4$  mM) of each mycotoxin in  $99.95\%$  CD<sub>2</sub>Cl<sub>2</sub> and  $99.96\%$  CDCl<sub>3</sub> were

transferred to an NMR tube. Dissolved oxygen was removed by a series of freeze-pump-thaw cycles on a vacuum line, and the tube was sealed.

NMR spectra were acquired at  $400$  MHz for <sup>1</sup>H and  $100$  MHz for <sup>13</sup>C on a Bruker DPX spectrometer with an Avance console and a single-axis gradient, inverse-detection probe. The residual solvent peak was used as a chemical shift reference. 1D <sup>1</sup>H NMR spectra, with and without selective homonuclear decoupling, were acquired with a sweep width of  $8278$  Hz and  $16k$  data points and the fid was zero-filled once. The resolution was enhanced with the application of a sine bell convolution function. Carbon  $T_1$  values were obtained using an inversion-recovery pulse sequence and a composite  $180^\circ$  pulse ( $90^\circ_x-180^\circ_y-90^\circ_x$ ). Proton chemical shifts and coupling constants for the  $2'-5'$  spin systems were obtained by fitting fully coupled and selectively decoupled spectra using version 2.5.2 of SpinWorks. Waltz proton-decoupled <sup>13</sup>C NMR spectra were acquired with a sweep width of  $23980$  Hz and  $64k$  data points and the fid was zero filled once. An analysis of the C-11' peak acquired with selective decoupling at the position of H-9' yielded <sup>3</sup>J<sub>H-C,4H</sub>. Upper bounds on several vicinal heteronuclear coupling constants for roridin A (Table 6) were obtained from a series of HMBC spectra. The intensity of the HMBC cross-peak depends on the value of <sup>3</sup>J<sub>C,H</sub>, whose variation is described by a Karplus equation. Maximum peak intensity is obtained when the  $d_6$  delay matches  $1/(2^3J_{C,H})$ . The delays employed— $30$ ,  $60$ ,  $90$ , and  $120$  ms—correspond to <sup>3</sup>J<sub>C,H</sub> of  $16.7$ ,  $8.3$ ,  $5.6$ , and  $4.2$  Hz, respectively. Small heteronuclear coupling constants, i.e., <sup>3</sup>J<sub>C,H</sub> <  $1$  Hz, were inferred from the systematic absence of the corresponding HMBC cross-peaks over the range of delays. Gradient-enhanced versions of COSY, ROESY, HMQC, and HMBC were employed. 2D spectra were acquired with a relaxation delay of  $2$  s, a sweep width of  $4200$  Hz in the proton dimension and  $22183$  Hz in the carbon dimension,  $1024$  data points, and zero filling in the  $t_2$  dimension. Apodization was applied in both dimensions: sine bell for COSY, squared cosine bell for ROESY and the proton dimensions of HMQC and HMBC, and exponential multiplication for the carbon dimensions of HMQC and HMBC. The number of  $t_1$  values was  $256$  for COSY, TOCSY, and ROESY and  $128$  for HMBC and HMQC. Zero filling was applied twice in the  $t_1$  dimension.

**Acknowledgment.** Financial support was from the Beckman Foundation and the Robbins Fund of Pomona College.

**Supporting Information Available:** <sup>1</sup>H and <sup>13</sup>C NMR spectra of roridin A and verrucaric acid, structural files of the three conformers in the Tripos mol2 format, and QSAR equations. This material is available free of charge via the Internet at <http://pubs.acs.org>.

## References and Notes

- (1) Augerson, W. A. *Review of the Scientific Literature As It Pertains to Gulf War Illnesses*; Rand Corp.: Santa Monica, CA, 2000; Chapter 4 in Vol. 5.
- (2) Wannemacher, R.; Wiener, S. *Medical Aspects of Chemical and Biological Warfare*; U.S. Government Printing Office: Washington, DC, 1997; Chapter 34 in Vol. TMM8.
- (3) Jarvis, B. B.; Mazzola, E. P. *Acc. Chem. Res.* **1982**, *15*, 388–395.
- (4) Wei, C. M.; McLaughlin, C. *Biochem. Biophys. Res. Commun.* **1974**, *57*, 838–844.
- (5) Boehner, B.; Tamm, C. *Helv. Chim. Acta* **1966**, *49*, 2527–2546.
- (6) Gutzwiller, A. J.; Tamm, C. *Helv. Chim. Acta* **1965**, *48*, 157–176.
- (7) Anderson, D. W.; Ashton, P. R.; Black, R. M.; Leigh, D. A.; Slawin, A. M. Z.; Stoddart, J. F.; Williams, D. J. *J. Chem. Soc., Chem. Commun.* **1988**, 904–908. CCDC Refcode: GESTON.
- (8) Soriano-García, M.; Ramos, F. M.; Chávez, G. T.; Ramírez-Medeles, M.; del, C.; Hernández, G. A.; Chicote, F. O. *Anal. Sci.* **1999**, *15*, 404–404. CCDC Refcode: GESTON01.
- (9) Jarvis, B. B.; Midiwo, J. O.; Flippen-Anderson, J. L.; Mazzola, E. P. *J. Nat. Prod.* **1982**, *45*, 440–448.
- (10) Breitenstein, W.; Tamm, Ch. *Helv. Chim. Acta* **1975**, *58*, 1172–1180.
- (11) Amagata, T.; Rath, C.; Rigot, J.; Tarlov, N.; Tenney, K.; Valeriote, F. A.; Crews, P. *J. Med. Chem.* **2003**, *46*, 4342–4350.
- (12) Shen, L.; Jiao, R. H.; Ye, Y. H.; Wang, X. T.; Xu, C.; Song, Y. C.; Zhu, H. L.; Tan, R. X. *Chem.-Eur. J.* **2006**, *12*, 5596–5602.
- (13) Berger, S.; Braun, S. *200 and More NMR Experiments*; Wiley-VCH: Weinheim, 2004.
- (14) Wüthrich, K. *NMR of Proteins and Nucleic Acids*; Wiley: New York, 1986.
- (15) Wüthrich, K. *Angew. Chem., Int. Ed.* **2003**, *42*, 3340–3363.

- (16) Steinmetz, W. E.; Sadowsky, J. D.; Rice, J. S.; Roberts, J. J.; Bui, Y. K. *Magn. Reson. Chem.* **2001**, *39*, 163–172.
- (17) Steinmetz, W. E.; Shapiro, J. J.; Roberts, J. J. *J. Med. Chem.* **2002**, *45*, 4899–4902.
- (18) Ladam, P.; Gharbi-Benarous, J.; Delaforge, M.; Van Calsteren, M.-R.; Jankowski, C. K.; Girault, J.-P. *Bioorg. Med. Chem.* **1995**, *3*, 587–604.
- (19) Gundertofte, K.; Liljefors, T.; Norrby, P.-O.; Petterson, I. *J. Comput. Chem.* **1996**, *17*, 429–449.
- (20) Hehre, W. J. *A Guide to Molecular Mechanics and Quantum Chemical Calculations*; Wavefunction: Irvine, CA, 2003.
- (21) Lynch, B. J.; Zhao, Y.; Truhlar, D. G. *J. Phys. Chem. A* **2003**, *107*, 1384–1388.
- (22) Cimino, P.; Gomez-Paloma, L.; Duca, D.; Riccio, R.; Bifulco, G. *Magn. Reson. Chem.* **2004**, *42*, S26–S33.
- (23) Steinmetz, W. E.; Pollard, J. E.; Blaney, J. M.; Winker, B. K.; Mun, I. K.; Hickernell, F. J.; Hollenberg, S. J. *J. Phys. Chem.* **1979**, *83*, 1540–1545.
- (24) Abragam, A. *Principles of Nuclear Magnetism*; Oxford University Press: Oxford, 1961; Chapter VIII.
- (25) Bystrov, V. F. *Russ. Chem. Rev.* **1972**, *41*, 281–304.
- (26) Hansch, C.; Leo, A. *Exploring QSAR*; ACS: Washington, DC, 1995.
- (27) Leo, A. J.; Hansch, C. *Perspect. Drug Discovery Des.* **1999**, *17*, 1–25.
- (28) Visconti, A.; Minervini, F.; Luciero, G.; Gamatesa, A. *Mycopathologia* **1991**, *113*, 181–186.
- (29) European Mycotoxin Awareness Network, <http://www.mycotoxins.org>.
- (30) Ouyang, Y. L.; Azcona-Olivera, J. I.; Pestka, J. L. *Toxicology* **1995**, *104*, 187–202.
- (31) CBInfo, <http://www.cbinfo.com/Biological/Toxins/TriToxicol.html>.
- (32) Hansch, C.; Steinmetz, W. E.; Leo, A. J.; Mekapati, S. B.; Kurup, A.; Hoekman, D. *J. Chem. Inf. Comput. Sci.* **2002**, *42*, 120–125.
- (33) Jarvis, J. B.; Stahly, G. P.; Pavanadasivam, G. *J. Med. Chem.* **1980**, *23*, 1054–1058.

NP070562X